A STRIP-YIELD MODEL FOR PREDICTING THE GROWTH OF PART-THROUGH CRACKS UNDER CYCLIC LOADING

Summary of Research
NASA Langley Research Center Grant NAG-1-2003

Principal Investigator:
Dr. S.R. Daniewicz
Department of Mechanical Engineering
Mississippi State University
662-325-7322
daniewicz@me.msstate.edu

NASA Technical Officer:
Dr. J. C. Newman, Jr.

6/22/00

RESEARCH OVERVIEW

Flaws exist in aircraft structures due to manufacturing operations and material defects. Under variable amplitude cyclic loading, these flaws grow as part-through cracks reducing the residual strength of structural components. To meet damage tolerant design requirements, accurate flaw growth predictions are needed which account for continual changes in crack shape as well as crack growth retardation and acceleration. Predicting the growth of part-through cracks under cyclic loading using an innovative and computationally efficient model is the focus of the research summarized in this report.

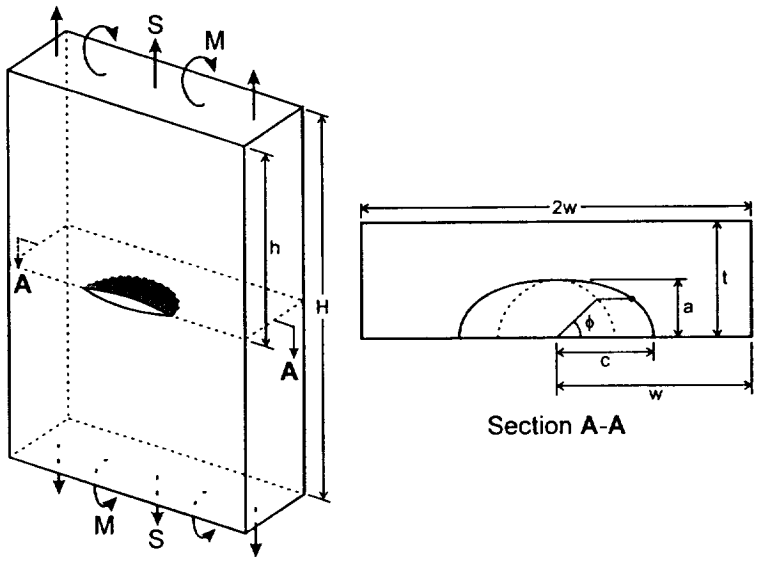

FIG. 1 Surface crack or part-through crack.

For through-cracks, both yield zone models and models based on plasticity-induced closure have been used to simulate crack growth under variable amplitude loading. Closure based models such as the modified strip-yield model incorporated within FASTRAN enable the prediction of crack growth behavior for a wide variety of load spectra without excessive empirical adjustment. Closure based models also allow consideration of small crack effects as recent studies suggest that closure plays a key role in the growth of small flaws. However, such models do not currently exist for the commonly encountered part-through crack shown in Fig. 1.

In this research effort, a slice synthesis methodology was developed and used to construct a modified strip-yield model for the part-through semi-elliptical surface flaw, enabling prediction of plasticity-induced closure along the crack front and subsequent fatigue crack growth under constant amplitude and variable amplitude loading. While modeling the plasticity-induced closure in a part-through flaw may be performed using three dimensional elastic-plastic finite element analysis, this type of effort is impractical from an engineering perspective. A modified strip-yield model similar to that used in FASTRAN for part-through flaws is a much needed engineering design tool, particularly when computational resources are limited. The model requires the following inputs:

1. material modulus, Poisson's ratio, and flow stress
2. crack growth rate material characterizations $da/dN = f(\Delta K_{eff})$ and $dc/dN = g(\Delta K_{eff})$
3. constraint factors at the deepest point of penetration α_A and the free surface α_B
4. plate width $2W$ and thickness t
5. distribution of applied stress in the uncracked plate
6. initial flaw size specification a and c
7. load history

With these inputs, the developed strip-yield model gives:
1. crack opening stresses at the deepest point of penetration and the free surface as a function of the number of applied cycles N
2. flaw depth a and length c as a function of the number of applied cycles N

The slice synthesis methodology used relies on approximate weight functions for two-dimensional slices which in turn approximate the three-dimensional surface crack geometry as illustrated in Fig. 2. The weight functions associated with the slices shown are approximated as an interpolation between a fixed condition with no displacement where the spring stiffness $k \rightarrow \infty$ and a free condition with $k \rightarrow 0$. To achieve the required interpolation, weight functions for both the free m_0 and fixed conditions m_∞ were needed, with the interpolation written as

$$m = m_\infty + \eta(m_o - m_\infty)$$

where η is a transition factor which varies form zero to unity. An expression of this type is required for both the a and c slices.

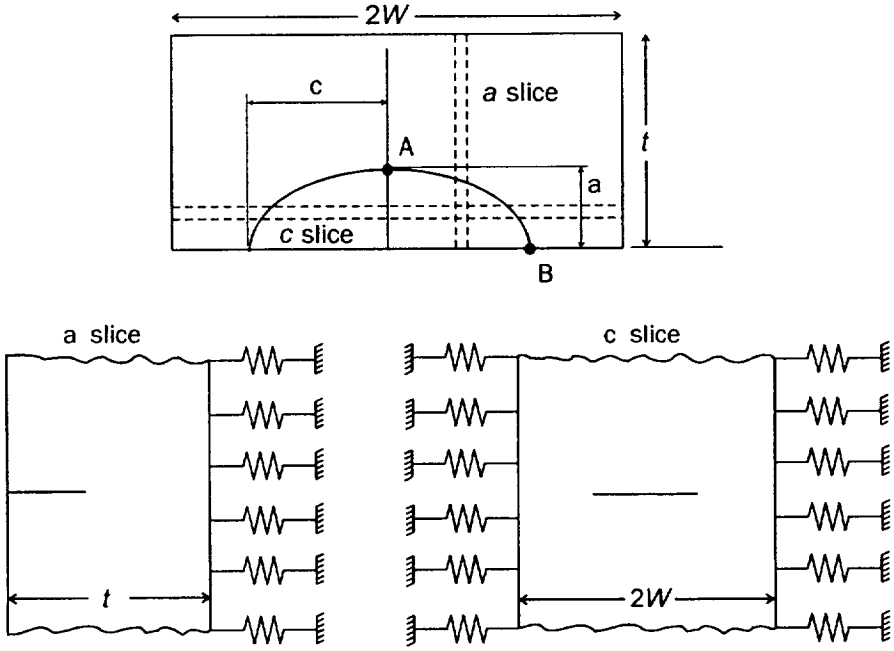

FIG. 2. Slice synthesis of surface flaw.

The transition factor for both the a and c slices was assumed to be a function of the normalized crack depth a/t, the aspect ratio a/c, and the normalized crack length c/W. Specific values of the transition factors were determined for prescribed a/t, a/c, and c/W by minimizing the following function using a downhill simplex method with simulated annealing

$$f(\eta_a, \eta_c) = (K_{ANR} - K_A)^2 + (K_{BNR} - K_B)^2$$

where K_{ANR} and K_{BNR} are the stress intensity factors at points A and B respectively on the crack front as computed using the Newman-Raju equations, while K_A and K_B are stress intensity factors as computed using the slice synthesis methodology with $K_A = K_A(\eta_a)$ and $K_B = K_B(\eta_c)$. The transition factors were tabulated for numerous a/T, a/c, and c/W, and a three-dimensional linear interpolation was used to extract the transition factor for a/t, a/c, and c/W values of interest.

The strip-yield model in its current state is limited to $a/t \leq 0.4$. The required weight function transition factors could not be successfully obtained for deeper cracks.

When using the strip-yield model, simplified variable amplitude loading may be considered in which the loading is defined as a sequence of constant amplitude blocks of loading of prescribed length N, maximum stress, and load ratio R. Note that this variable amplitude loading is much less general than that allowed in FASTRAN.

Details and numerous results obtained from the strip-yield model can be found in references (1), (2), (3), (6), and (8).

SUMMARY OF RESULTS

Constraint Characterization

When using modified strip-yield models, it is assumed that the stress within the plastic zone is a constant. The stress σ_{yy} in the plastic zone will actually be nonuniform due to constraint effects as well as strain hardening. A constraint factor is used to approximate this nonuniform stress. The constraint factor α describes the average stress to flow stress ratio in the plastic zone. At the deepest point of flaw penetration, a plane strain condition exists and a large constraint factor will result. At the free surface, a plane stress condition exists and a smaller constraint factor will be observed.

Elastic-plastic finite element analyses of surface-cracked plates were performed using the commercial finite element code ANSYS. Various crack geometries were analyzed under tension and bending loads. A constraint factor dependent on the location along the perimeter of the surface crack was computed. This constraint factor was the averaged normal stress to flow stress ratio acting on a line originating on and perpendicular to the crack front at a prescribed location and terminating at the perimeter of the plastic zone on the crack plane.

The finite-element meshes were generated using a FORTRAN code *mesh3d_scpcell* written by J. Faleskog (Royal Institute of Technology, Stockholm, Sweden). The size of the models used

ranged from about 33,500-51,500 nodes and 30,000-46,400 eight-noded hexahedral elements. A typical model is shown in Fig. 3. It should be noted that roughly two years of experience with this mesh generation code has revealed that the software has difficulty when large degrees of refinement are attempted, with poor element aspect ratios resulting in transition regions.

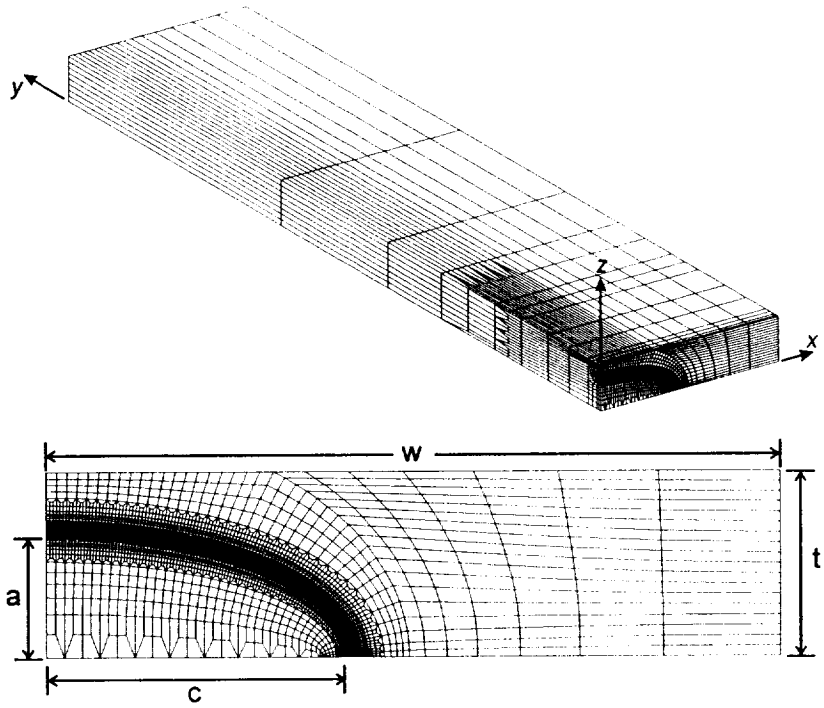

FIG. 3. Typical finite-element model of surface-crack configuration

The constraint factor α is the average of the normal opening mode stress, σ_{yy}, acting along a "ray" perpendicular to the crack front of the yielded elements. The constraint factor is defined as

$$\alpha(\phi) = \frac{1}{A_r(\phi)} \sum_{n=1}^{N(\phi)} (\sigma_{yy}/\sigma_o)_n A_n$$

where A_n is the projected area of the yielded element n on the crack plane, $(\sigma_{yy}/\sigma_o)_n$ is the normalized centroidal stress perpendicular to the crack plane for element n, and $A_r(\phi)$ is the total projected area for all yielded elements along a given ray, $N(\phi)$. Yielded elements were defined by a non-zero equivalent plastic strain. Each ray of elements were defined by the parametric angle, ϕ, along the crack front. This angle was calculated at the midpoint of the two nodes of each element immediately adjacent to the crack front.

Fig. 4 show some typical constraint variations along the crack front for different crack configurations subjected to remote bending and tension. The constraint is near unity (plane stress) at the free surface, as expected, and rises at the maximum depth location ($\phi = 90°$). Details may be found in references (4) and (7).

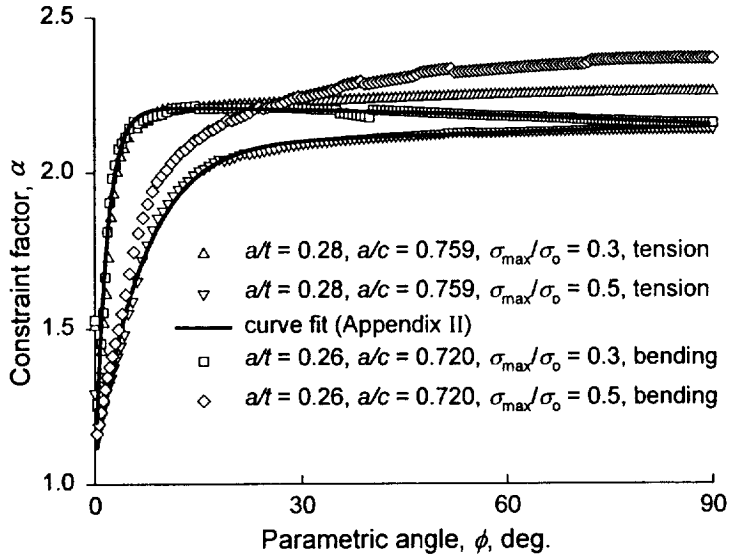

FIG. 4. Typical constraint factor variation.

Verification of Surface Flaw Modified Strip-Yield Model

The strip-yield model for the surface flaw was partially verified by comparing monotonic plastic zone sizes and crack surface displacements with those computed from detailed elastic-plastic 3D finite element results as seen in Fig. 5. Crack surface displacements from the model were shown to compare well with results from three-dimensional elastic-plastic finite element analyses.

When looking at the plastic zone on the crack plane, the plastic zone was observed to be largest beneath the free surface as shown in Fig. 6. However, viewing the crack front plastic zone on the crack plane alone results in an unrealistic perspective of crack front plasticity. A three-dimensional view of the part-through flaw plastic zone along the crack front revealed yielding on the crack plane is highly restricted when compared to regions off of the crack plane as shown in Fig. 7. For more detail see reference (8).

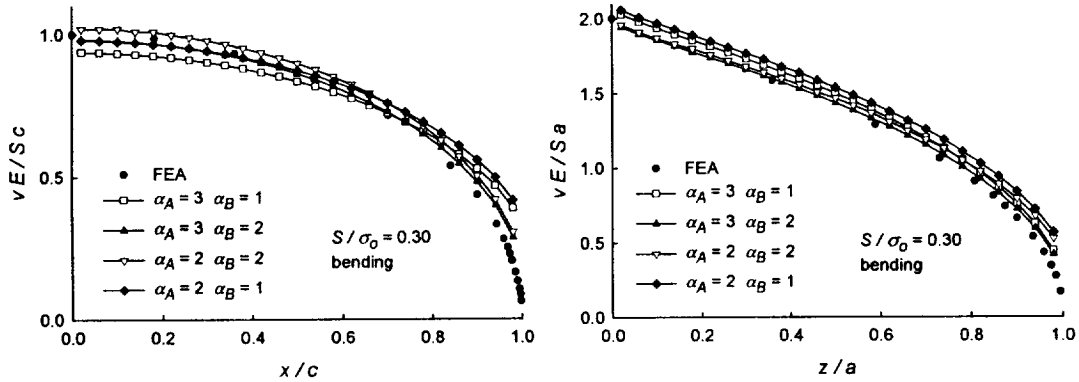

FIG. 5. Typical crack surface displacement comparison.

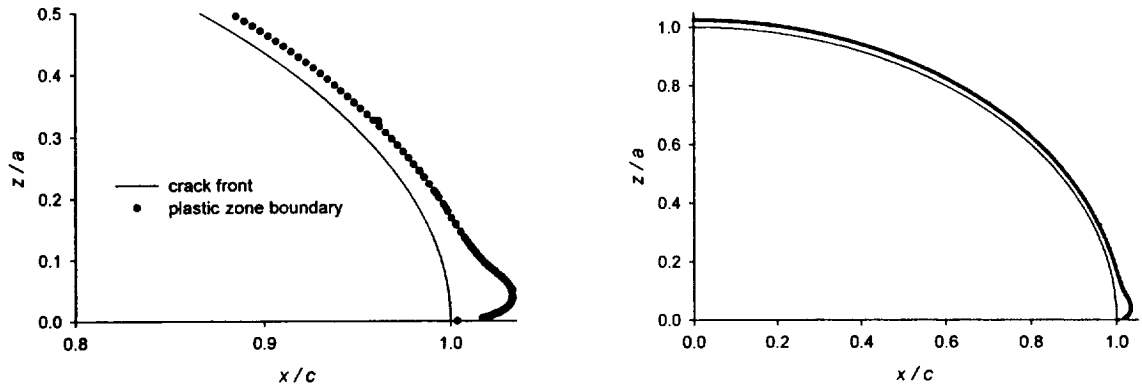

FIG. 6. Typical plastic zone variation along crack front in the crack plane.

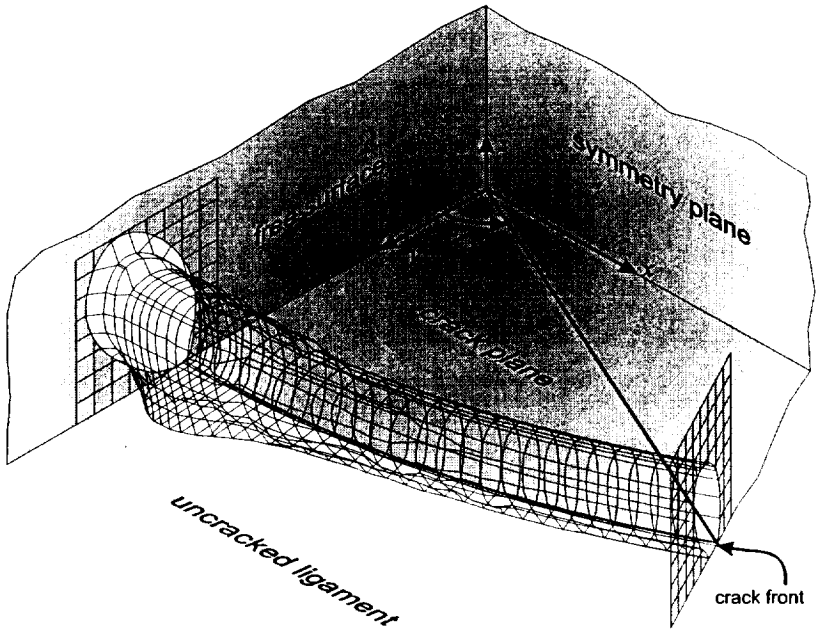

FIG. 7. Typical plastic zone near the free surface.

Characterization of Fatigue Crack Growth Behavior for AA 7075-T6

To verify the strip-yield model, experimental data describing the growth of surface cracks under cyclic loading was needed. 7075-T6 aluminum plate with a thickness of 0.50 inches was purchased for testing purposes. From this plate, surface crack fatigue crack growth specimens were machined as shown in Fig. 8. Multiple fatigue tests were conducted under constant amplitude loading with a stress ratio $R = 0.1$, which inherently included the effects of fatigue crack closure, and $R = 0.7$, which was assumed closure free. Crack length measurements on the

free surface were made with a traveling microscope. To allow crack depth measurements, marker bands were used.

The aspect ratio evolutions for the two stress ratios tested were compared to determine whether crack closure affects aspect ratio or crack shape evolution. It was found that closure impacts this evolution in a significant manner as shown in Fig. 9. The observed crack growth rate-stress intensity factor range relationships for $R = 0.7$ at the free surface and the deepest point of penetration were compared to existing through-crack data, with a good correlation being observed as shown in Fig. 10.

In addition, the fatigue crack growth data collected from the multiple specimens was used to perform uncertainty analyses on the crack lengths, crack depths, and the aspect ratio. This was done to determine if crack growth models are best validated using the aspect ratio as the measured quantity or the individual measured crack length and crack depth. The measured aspect ratio was found to exhibit a smaller percentage of experimental uncertainty, and thus should be used for model validations. Details can be found in reference (9).

The idea of a single intrinsic curve such as that shown in Fig. 10 for a given material in a given environment is an integral part of fatigue crack growth prediction methodologies incorporating crack closure concepts. The existence of such a curve has come into question, as recent research has suggested that da/dN is a function of both ΔK_{eff} and the maximum stress intensity K_{max}.

During the next stage of the research, which is currently underway, fatigue crack growth rate will be measured in AA 7075-T6 compact tension specimens under both K_{max} control and load control allowing determination of da/dN as a function of ΔK_{eff} in both the Paris regime and the threshold regime. In the threshold and near threshold regime, load shedding with multiple fixed K_{max} levels will be used to ascertain effects of K_{max} on the da/dN - ΔK_{eff} curve. In the Paris regime, opening load measurement will be improved using a newly developed smoothing operation as discussed in reference (5). Given that the fatigue crack growth process is highly stochastic in nature, multiple tests will be performed using each of the K_{max} values, and a detailed experimental uncertainty analysis will be performed. This will allow uncertainty bands for the data to be established. Any observed K_{max} effects can only be considered significant if a change in K_{max} produces data outside the uncertainty bands.

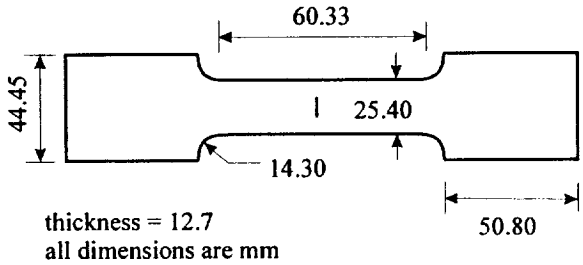

FIG. 8. Surface crack fatigue crack growth specimen.

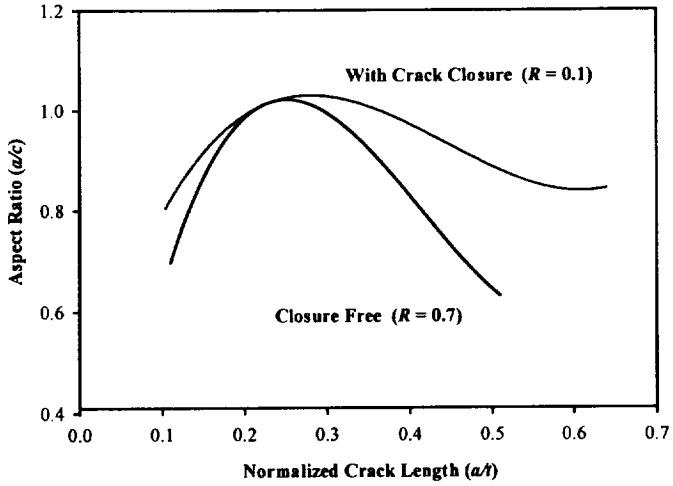

FIG. 9 Aspect ratio evolution.

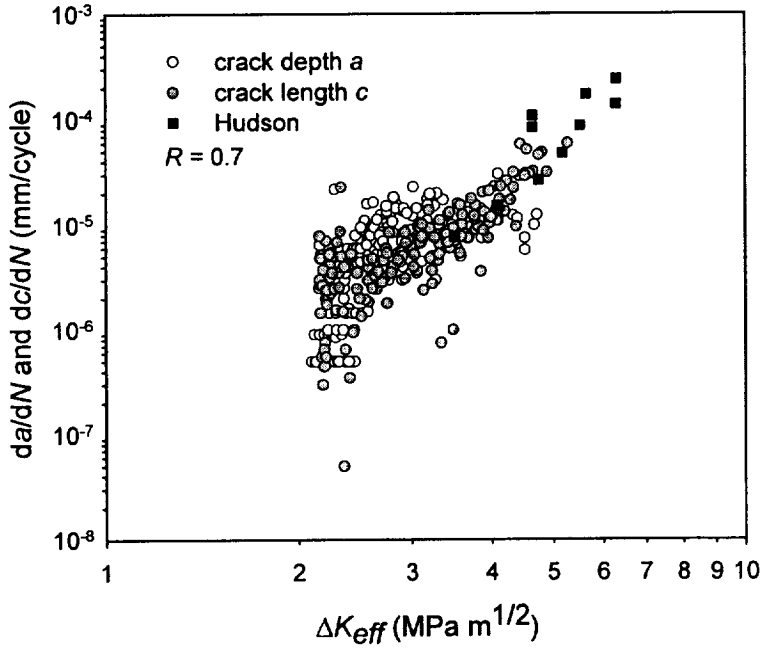

FIG. 10. AA 7075-T6 fatigue crack growth rate for through-cracks and surface cracks.

Modeling Growing Surface Flaws Using Three-Dimensional Elastic-Plastic Finite Element Analysis

Crack opening stresses for surface cracks were also predicted using finite element analyses to allow comparison with the strip-yield model. This effort is not yet completed. Crack opening levels were determined for two different surface crack models using ANSYS. The first surface crack model was a semi-circular crack with an aspect ratio, $a/c = 1$. The second model was a semi-elliptical surface crack with an aspect ratio, $a/c = 0.5$.

The semi-circular model shown in Fig. 11 was used to determine the effects of various solution options. Three different solution options were studied: the loading increment, the iterative solver tolerance, and the use of the non-linear geometry (large deformation) option. The model used a relatively coarse mesh, so high stress levels ($S_{max} / \sigma_o = 0.7$) were required to ensure adequate refinement in the plastic zone. At the maximum load, the model had 15 elements in the plastic zone at the crack deep point, and 33 elements in the plastic zone near the free surface. The mesh had a total of 31,392 nodes and 27,768 elements. The crack opening levels along the crack front were determined after 10 crack growth cycles. Four analyses were run with this mesh to determine the best solution options. All four analyses resulted in the same opening levels along the crack front (Fig. 12), so solution time can be used to determine the best options. The solution options and time are shown in the table below. It can easily be seen from these results that the best solution options in terms of time should be with a loading increment of 5% of the load range, a solver tolerance of 1E-4, and large deformation effects off. A final analysis will be run with these options used together to insure there is no effect on the crack opening levels.

	Load Increment	PCG Solver Tolerance	Large Deformations	Solution Time (hours)
Case 1	2.5%	1E-8	OFF	71
Case 2	5%	1E-8	OFF	48.5
Case 3	2.5%	1E-4	OFF	57
Case 4	2.5%	1E-8	ON	92

A semi-elliptical model shown in Fig. 13 was used to compare finite element results with published experimental results. The model geometry was chosen to match a specimen tested by Putra and Schijve. A large model was required to ensure adequate mesh refinement in the plastic zone. At maximum load there were 10 elements in the plastic zone at the crack deep point. The mesh contained 59,493 nodes and 53,804 elements. Since the model was so large, the crack opening levels were determined after only 5 crack growth cycles. Because the crack was grown only 5 cycles, the opening levels at the free surface did not stabilize, but this is not of too much concern since opening levels near the free surface were not reported by Putra and Schijve. The opening levels for the crack interior as determined by FEA are much higher than those determined experimentally as seen in Fig. 14. This effort is currently continuing.

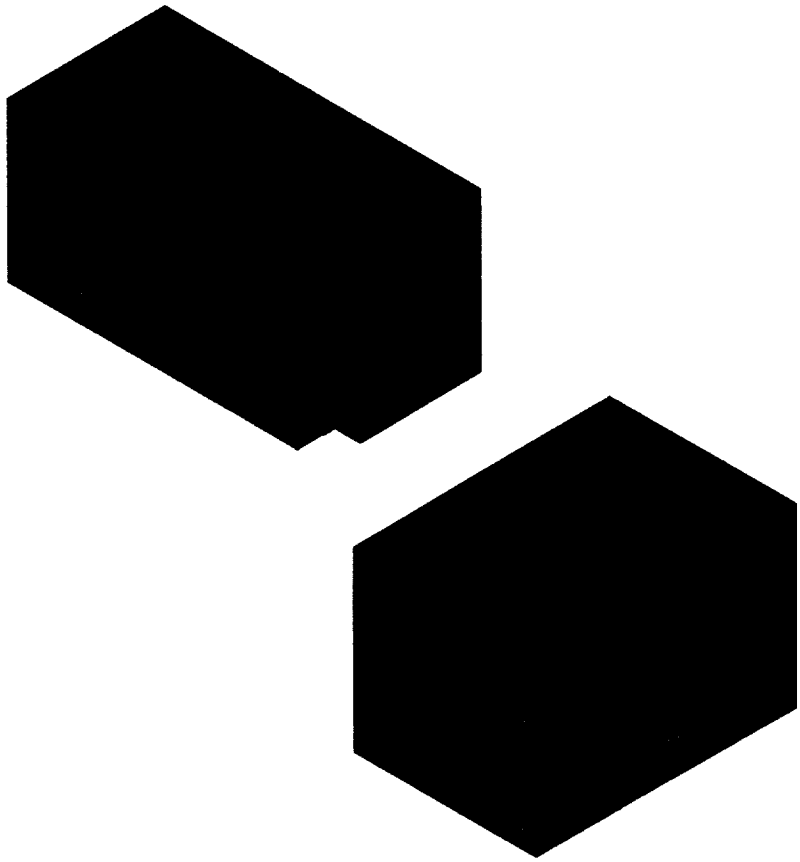

Fig. 11. Semi-circular crack mesh.

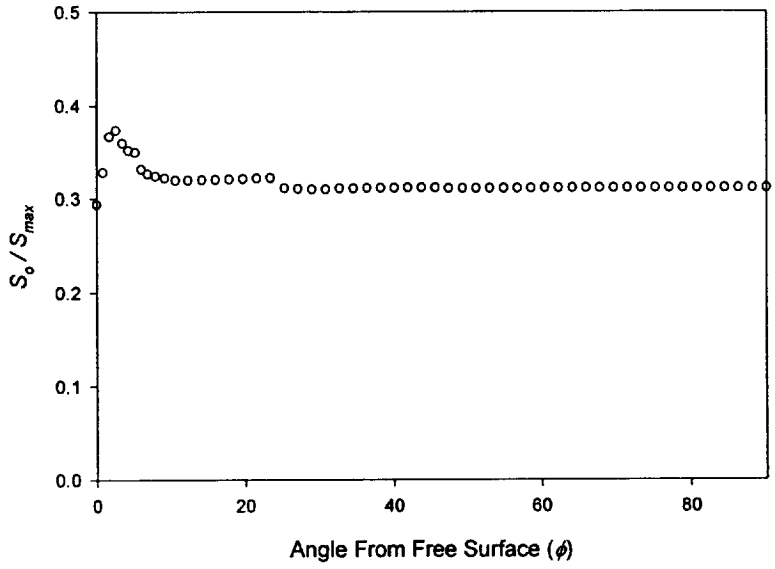

FIG. 12. Predicted crack opening stress for semi-circular crack.

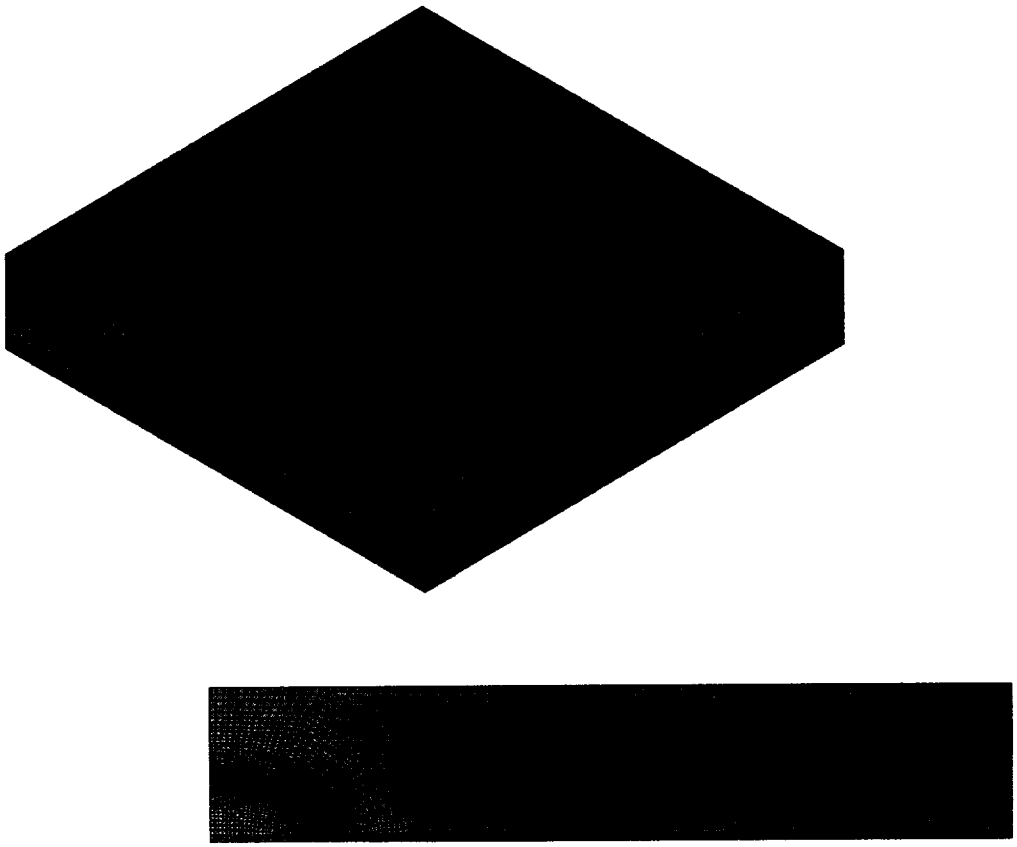

FIG. 13. Semi-elliptical crack mesh.

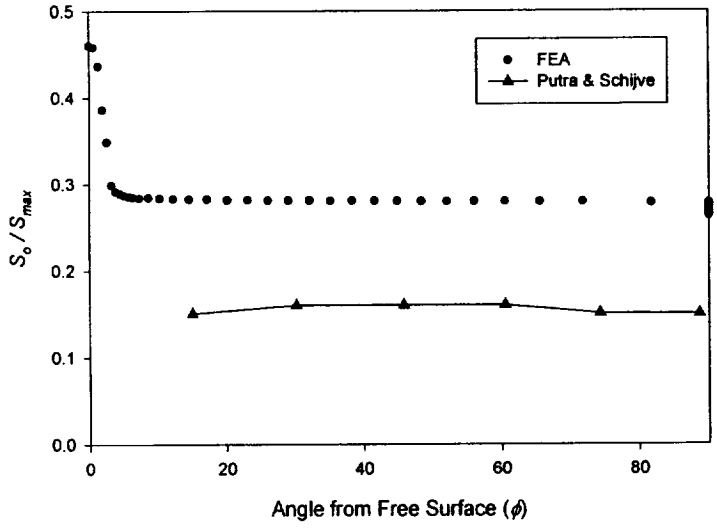

FIG. 14. Predicted and measured crack opening stresses

REFERENCES

1. Daniewicz, S. R., "A Modified Strip-Yield Model for Prediction of Plasticity-Induced Closure in Surface Flaws," *Fatigue and Fracture of Eng. Materials and Structures*, Vol. 21, 1998, pp. 885-901.

2. Daniewicz, S. R., "Prediction of Plasticity-Induced Closure in Surface Flaws Using a Modified Strip-Yield Model", ASTM STP 1332, 1999, pp. 453-473.

3. Daniewicz, S. R., "Evaluating the Influence of Plasticity-Induced Closure on Surface Flaw Shape Evolution Under Cyclic Loading Using a Modified Strip-Yield Model," ASTM STP 1343, 1999, pp. 393-410.

4. Newman, J. C., Reuter, W. G., and Aveline, C. R., "Stress and Fracture Analyses of the Surface Crack," ASTM STP 1360, 1999.

5. Daniewicz, S. R., "Smoothing And Differentiating Load-Displacement Data Using A Low Pass Filter For Improved Crack Opening Load Estimates," *Fatigue and Fracture of Eng. Materials and Structures*, Vol. 22, No. 4, 1999, pp. 273-280.

6. Daniewicz, S. R. and Aveline, C. R., "A Strip-Yield Model for Part-Through Surface Flaws Under Monotonic Loading," ASTM STP 1389, 1999.

7. Aveline, C. R. and Daniewicz, S. R., "Variations of Constraint and Plastic Zone Size in Surface-Cracked Plates Under Tension and Bending Loads," ASTM STP 1389, 1999.

8. Daniewicz, S. R. and Aveline, C. R., "Strip-Yield and Finite Element Analysis of Part-Through Surface Flaws," accepted for publication *Eng. Fracture Mech.*, April, 2000.

9. McDonald, V. and Daniewicz, S. R., "An Experimental Study of the Growth of Surface Flaws Under Cyclic Loading: Experimental Uncertainty, Aspect Ratio Evolution, and the Influence of Crack Closure," ASTM STP 1406, 2000.